Accepted Manuscript

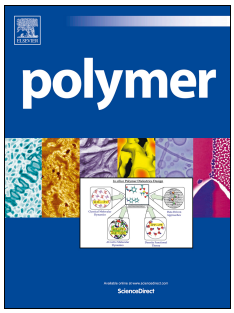

Fuel cell electrolyte membranes based on copolymers of protic ionic liquid [HSO_3-BVIm][TfO] with MMA and hPFSVE

V.M. Ortiz-Martínez, Alfredo Ortiz, Verónica Fernández-Stefanuto, Emilia Tojo, Maxime Colpaert, Bruno Améduri, Inmaculada Ortiz

PII: S0032-3861(19)30567-1

DOI: https://doi.org/10.1016/j.polymer.2019.121583

Article Number: 121583

Reference: JPOL 121583

To appear in: *Polymer*

Received Date: 24 January 2019

Revised Date: 10 May 2019

Accepted Date: 14 June 2019

Please cite this article as: Ortiz-Martínez VM, Ortiz A, Fernández-Stefanuto Veró, Tojo E, Colpaert M, Améduri B, Ortiz I, Fuel cell electrolyte membranes based on copolymers of protic ionic liquid [HSO_3-BVIm][TfO] with MMA and hPFSVE, *Polymer* (2019), doi: https://doi.org/10.1016/j.polymer.2019.121583.

Graphical Abstract

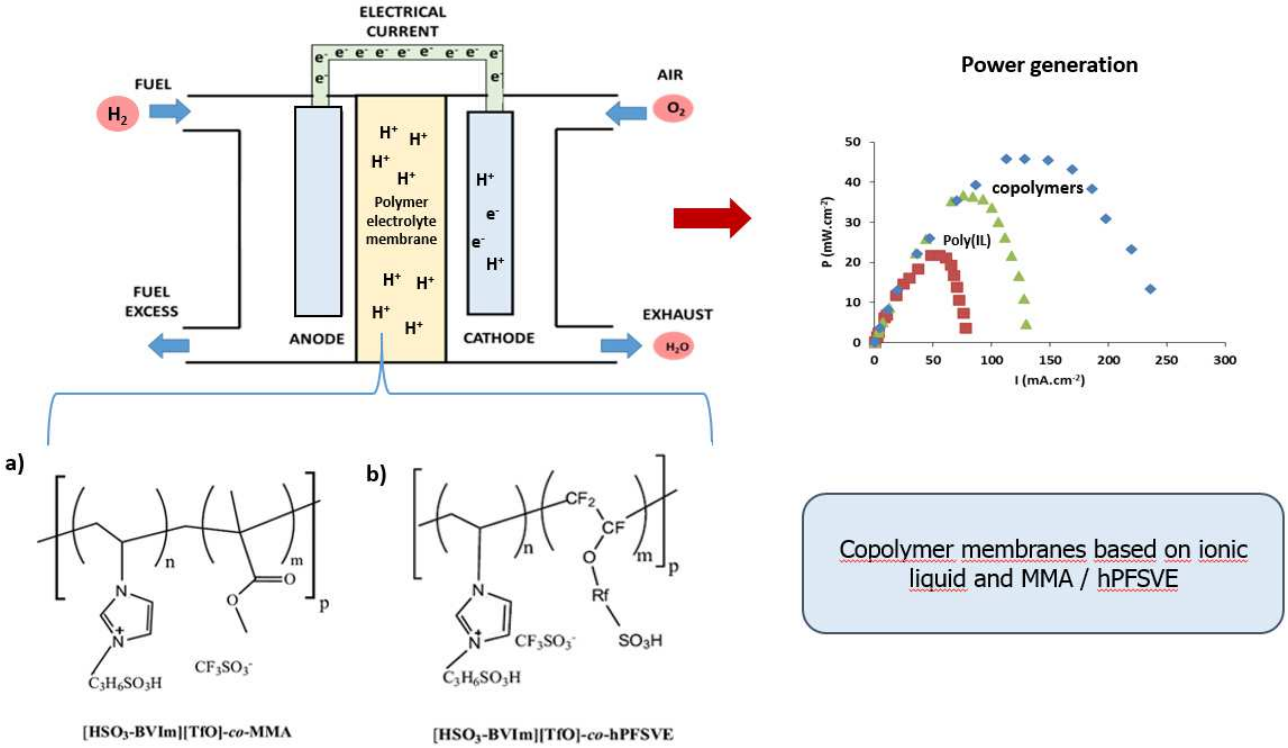

Copolymer membranes based on ionic liquid and MMA / hPFSVE

Fuel cell electrolyte membranes based on copolymers of protic ionic liquid [HSO_3-BVIm][TfO] with MMA and hPFSVE

V.M. Ortiz-Martínez[a], Alfredo Ortiz[a], Verónica Fernández-Stefanuto[c], Emilia Tojo[c], Maxime Colpaert[b], Bruno Améduri[b], Inmaculada Ortiz[a,*]

[a]*Department of Chemical and Biomolecular Engineering, University of Cantabria, Av. Los Castros 46, 39005 Santander, Spain.*

[b]*ICGM – Ingénierie et Architectures Macromoléculaires, UMR 5253 CNRS, Université de Montpellier, ENSCM, Place Eugène Bataillon, 34095 Montpellier Cedex 5, France*

[c]*Department of Organic Chemistry, University of Vigo, 36210-Vigo, Spain*

*Corresponding author: ortizi@unican.es

Abstract

Polymeric ionic liquids (PILs) have recently been attracting great attention as new types of electrolytes for polymer exchange membrane fuel cells (PEMFCs), clean energy devices, due to their outstanding properties. In this work, the copolymerization of the ionic liquid (IL) 1-(4-sulphobutyl)-3-vinylimidazolium trifluoromethanesulphonate, [HSO_3-BVIm][TfO], with methyl methacrylate (MMA) and perfluoro-3,6-dioxa-4-methyl-7-octene sulfonyl fluoride in its hydrolyzed form (hPFSVE), respectively, was performed for the preparation of structurally new IL copolymer membranes with enhanced conductive properties in comparison with the pristine PIL form. Membranes were synthesized through a facile photopolymerization method under UV radiation. The effect of temperature under wet and dry conditions on the ionic conductivities of the resulting membranes was analyzed. The performances of the new membranes were also assessed in a proton exchange fuel cell for power generation. Both poly([HSO_3-BVIm][TfO]-*co*-MMA) and poly([HSO_3-BVIm][TfO]-*co*-hPFSVE) electrolyte membranes offered high conductivity even in dry conditions (in the order 10^{-3} - 10^{-2} S·cm^{-1}). At low MMA and hPFSVE amounts (10 mol%), the ionic conductivity and power performances of the resulting membranes were enhanced in comparison with the membrane only

constituted of the polymerizable IL showing the promising prospects of these ionic liquid-based copolymers as proton exchange membranes, with power outputs up to 45 $mW.cm^{-2}$.

Keywords: copolymerization; ionic liquid; fuel cell.

1. Introduction

In a society where increasing amounts of energy are being demanded, proton exchange membrane fuel cells (PEMFCs) are among the most promising options for efficient and clean energy generation. These sustainable energy devices are capable of converting directly chemical energy into electricity with zero CO_2 emissions [1]. Fuel cells are inherently modular and of static nature, which delivers significant benefits in terms of construction and applications for portable, stationary and transportation power generation. Due to the advantages of PEMFCs, this technology has been intensively investigated in the last decades and is already in the early stage of commercialization [2–5].

Proton exchange membranes are the core of PEMFCs and thus, they have significantly progressed through the development of new and enhanced polymer materials [6–11]. Hydronium cations migrate from the anode to the cathode through a proton-conducting electrolyte while electrons are led to the cathode through an external circuit. At the cathode, oxygen is supplied as electron acceptor (in air form or as pure oxygen). The overall process results in the combination of hydrogen and oxygen to produce water, heat and electricity. Ideal fuel cell polymer membranes should display high proton conductivity (even in dry conditions) and low electronic conductive while avoiding fuel crossover. In addition, they should offer chemical and thermal stabilities, reasonable mechanical properties and low manufacture costs.

So far, perfluorinated sulphonic acid (PFSA) membranes such as Nafion®, Fumion®, Flemion®, Aquivion® and 3M™ membranes, have been the most common membranes used in fuel cell systems due to their high performances and lifetime [12,13]. Nevertheless, several non-fluoridated polymer alternatives have been developed to overcome the drawbacks inherent to PFSA membranes, mainly high cost, high gas crossover and efficient operation restricted to anhydrous conditions. Some of these alternative polymer options include polybenzimidazole doped with phosphoric acid [14,15], sulfonated polyimides [16,17], polyphosphazenes [18], sulfonated polystyrene composites [19], polyethersulfone and sulfonated poly(ether-ether-ketone) [20], as well as natural polymer and bioinspired membranes [21]. However, most of these non-fluorinated polymers exhibit some oxidation decomposition issues [22] or, in case of natural polymers, need further improvements to obtain higher levels of power generation.

A different and recent approach consists in developing polymeric ionic liquid (IL) membranes for their use in PEMFCs [23]. Room temperature ionic liquids (RTILs) are organic salts remaining liquid at ambient temperature which display outstanding properties such as high ionic conductivity both in hydrous and anhydrous conditions, high long-term chemical and thermal stabilities, extremely low vapor pressure and wide electrochemical stability window [24–27]. All these properties make these compounds ideal candidates as membrane electrolytes in fuel cells. However, as RTILs are in the liquid state, they pose a challenge since thin and solid membranes are needed for set-up and operation. Thus, several strategies to manufacture ionic liquid-based membranes have been reported and mainly consist of (i) incorporating ILs into a polymer network by mixing both phases, typically by casting techniques, or (ii) forming solid membranes through the polymerization of IL monomers. RTILs containing imidazolium cations have been widely studied for electrochemical applications since they have been reported to offer higher overall ionic conductivities compared to RTILs based on other types of

cations (e.g. tetraalkylammonium, tetraalkylphosphonium, pyridinium, pyrrolidinium). RTILs with dialkylimidazolium cations are typically characterized by ionic conductivities in the order of 10^{-2} S.cm^{-1} while the ionic conductivities displayed by ILs based on the aforementioned cations are well below this order of magnitude (10^{-4} - 10^{-3} S.cm^{-1}) [23,24].

The mixing of ILs with other polymer materials leads to enhanced ionic transport due to the modification of the ion dissociation degree, transition temperature (T_g) of the resulting membrane and moiety concentration [28]. Several examples reported in the literature include the impregnation of SPEEK membranes with the 1-butyl-3-methylimidazolium tetrafluoroborate IL [29], the combination of poly(vinylidene fluoride-*co*-hexafluoropropylene) copolymer with ILs containing the trifluoromethylsulfonate anion, [TfO], [30] or the incorporation of 1-H-3-methylimidazolium bis(trifluoromethanesulfonyl)imide (imbedded in commercial zeolites) into PBI membranes [31], with resulting conductivities varying from 2 to 54 mS.cm^{-1} at high temperature (>140 ºC). This technique often results in a trade-off between the desirable RTIL properties and the mechanical strength of the membranes and can induce leakage issues. In fact, when assessed in fuel cell devices, power performance reported for these electrolyte membranes in intermediate and high temperature fuel cells was relatively low (e.g. 1.2 mW.cm^{-2} at 110 ºC [30]).

Polymerization of ILs results in the formation of ionic polymers, which are known as poly(ionic liquid)s or polymeric ionic liquids (PILs) [32]. PILs can be synthesized through reversible deactivation radical polymerization (RDRP) techniques such as atom transfer radical polymerization and reversible addition fragmentation chain transfer polymerization, which have been employed for the preparation of homopolymers and block copolymers [33–38]. An attractive alternative to RDRP methods consists of the photopolymerization of ILs to prepare PILs since this technique provides short synthesis

times, ease of control and can be achieved at room working temperature [39]. Vinyl, vinylbenzyl and methacryloyl groups are usually targeted as the polymerizable groups covalently attached to the cationic sites [39,40]. Polymerization of IL monomers leads to the reduction of the ionic conductivities as a result of reduced ion mobility and a higher T_g. While the conductivity of ILs remains in the order of 10^{-2} S. cm^{-1}, PILs can display conductivities in the order of 10^{-6} S.cm^{-1}. However, PILs result in single-ion conductors suitable for ion exchange membranes in electrochemical devices. In a previous work [41], the addition of bulk non-polymerizable IL into the structure of PILs was addressed to increase the ionic conductivity of PILs by maintaining the fluidity of the electrolyte. Specifically, the addition of the non-polymerizable IL 1-(4-sulphobutyl)-3-methylimidazolium trifluoromethanesulphonate, [HSO_3-BMIm][TfO], into a polymeric matrix of the polymerizable 1-(4-sulphobutyl)-3-vinylimidazolium trifluoromethanesulphonate IL, [HSO_3-BVIm][TfO], notably improved both ionic conductivity of the resulting composites and power performance in PEMFCs.

In a new strategy, this work aims at preparing IL membranes with enhanced conductive properties in comparison with the pristine PIL membrane. Specifically, the crosslinking copolymerization of the polymerizable IL [HSO_3-BVIm][TfO] with methyl methacrylate (MMA) and perfluoro-3,6-dioxa-4-methyl-7-octene sulfonyl fluoride in its hydrolyzed form (hPFSVE), respectively, is approached for the first time to process polymer electrolyte membranes. The effect of temperature under wet and dry conditions on the ionic conductivity of the resulting membranes was studied. The performances of the new membranes were also assessed in PEMFCs for power generation.

2. Experimental

2.1. Materials

2-Hydroxy-2-methylpropiophenone (97%), glycerol dimethacrylate (85%) and methyl methacrylate (MMA) (99%) were purchased from Sigma-Aldrich (Germany). The ionic liquid 1-(4-sulphobutyl)-3-vinylimidazolium trifluoromethanesulphonate ([HSO_3-BVIm][TfO]) was synthesized according to the method previously reported [30]. Briefly, the synthesis process consists of the quaternization reaction between 1-vinylimidazole and 1,4-butane sultone with subsequent treatment with triflic acid (TfOH) in acetonitrile (reactant purities of >99%, Sigma-Aldrich, Germany). The fluorinated monomer, perfluoro-3, 6-dioxa-4-methyl-7-octene sulfonyl fluoride (PFSVE), was hydrolyzed to convert SO_2F groups into sulfonic acid functions (hPFSVE) and then was then employed for membrane synthesis according to a previous method [42].

2.2. Polymerization

Membranes were fabricated via in situ photopolymerization by mixing a certain quantity of the polymerizable [HSO_3-BVIm][TfO] IL with x mol% of MMA (x=5, 10 for MMA) or the fluorinated monomer hPFSVE (x= 10, 20, 30, 40 for hPFSVE), along with 5 wt% of crosslinker (glycerol dimethacrylate) and 2 wt% of photoinitiator (2-hydroxy-2-methyl propiophenone). The resulting slurry was uniformly spread over a glass surface and directly exposed to UV light using a KAIS curing oven (KGW-94N, 30 mW/cm^2 at 365 nm) for 30 min. After polymerization, the membranes were left overnight to facilitate their separation from the glass surface. During the process, all the starting mixture was converted into a flat solid membrane and the proper size was cut for fuel cell test (5 cm^2). Additional membranes based only on ionic liquid (in the absence of methacrylic/fluorinated monomer) were also synthesized for comparison purposes. Membrane thickness was measured with a Mitutoyo (Japan) micrometer (1 µm of accuracy).

2.3. Analysis

The morphology appearance of membrane samples was analyzed using a Zeiss EVO MA15 scanning electron microscope (SEM) and energy dispersive X-ray (EDX) for mapping analysis (Oxford Instruments). The photopolymerization process was confirmed with attenuated total reflection Fourier transform infrared spectroscopy (ATR-FTIR) within the wavenumber range 400-4000 cm^{-1} using a PerkinElmer Spectrum 65 FT-IR Spectrometer with a coupled ATR unit (GladiATR, resolution of 2 cm^{-1}). The thermal stability of the synthesized membranes was studied with thermogravimetric analysis (TGA) employing a Shimadzu TGA-60H series analyzer from ambient temperature to 500 ºC (heating rate of 10 $ºC.m^{-1}$) in an inert nitrogen environment.

The weight of membrane samples were monitored before and after being washed with water to study possible weight losses. To this end, membrane samples were first dried under vacuum (60 ºC, 33 mbar for 3 h) and then washed with water at 20 ºC and dried under same conditions. On the other hand, water uptake was calculated with new samples according to the following procedure: the resulting polymerized membranes were first dried under vacuum (60 ºC, 33 mbar for 3 h) and then immersed in water for 24 h at 20 ºC. The membranes were weighed before and after immersion and water uptake was calculated as follows:

$$\text{Water uptake (\%)} = = \frac{m_{wet} - m_{dry}}{m_{dry}} \text{ x } 100$$

where m_{wet} and m_{dry} stand for the masses of the wet and dry membrane samples, respectively.

In order to analyze the influence of temperature, humidity, the IL content and the nature of the monomer on the ionic conductivity, the electrochemical impedance spectroscopy (EIS) technique was employed to study the conductivity of the membranes under dry and wet conditions. For dried conditions, membranes were dried under vacuum (33 mbar) at 60 ºC for 3 hours and their ionic conductivity was measured. For wet conditions,

membrane samples were immersed in water to become wet before EIS measurements. EIS tests were performed with a Zahner-elektrik IM6 workstation in potentiostatic mode with amplitude of 10 mV in the frequency range from 1 Hz to 1 MHz. EIS measurements were recorded *ex situ* in a homemade cell specifically designed to this purpose, which consists of two stainless steel rods between which round membrane pieces of 1.26 cm of diameter were placed. Measurements were performed from room temperature to 90 ºC by placing the cell inside a conventional oven with temperature control. The data were both collected and analyzed with *Thales* software from Zahner-elektrik (Germany) to obtain Bode plots [43]. Membrane conductivity was calculated as $\sigma = R / (L \cdot A)$, in which σ, R, L and A stand for membrane conductivity ($S.cm^{-1}$), ohmic resistance (Ω) obtained from Bode plots, membrane thickness (cm) and membrane area (cm^2), respectively.

2.4. Fuel cell performance

The experimental set-up employed for the assessment of the fuel cell performances of the synthesized membranes is represented in Figure 1. Membranes were tested in a commercially available PEM fuel cell stack (quickCONNECT- balticFuelCells GmbH, Germany). The fuel stack includes anodic and cathodic graphite plates and serpentine flow fields of 5 cm^2 of active area. Polymerized membranes were placed between gas diffusion electrodes with catalyst loading of 0.5 mg $Pt.cm^{-2}$ (balticFuelCells GmbH, Germany). The PEMFC system is equipped with a pressure controlled clamping force system (pneumatic actuator) to ensure good contact between the internal components of the cells. Anode compartment was fed with pure hydrogen (fuel) at a flow rate of 320 $mL.min^{-1}$, while the cathode compartment was fed with air for oxygen supply at 500 $mL.min^{-1}$, both at a fixed feeding pressure of 1.5 bar. The tests were performed using humidified gases to study the behavior of the membranes at optimal conditions according to the results obtained from ionic conductivity measurements. For this purpose, hydrogen and air streams were passed through bubblers containing water at a

temperature of 80 ºC with resulting relative humidity of 100 %. To avoid water condensation in gas streams after bubblers, gas line temperatures were controlled (Figure 1). In order to obtain polarization curves (I-V), an electronic load was connected to the fuel cell stack for the stepwise reduction of the potential from open-circuit voltage (OCV) to nearly short circuit. Power density curves (I-P) were accordingly calculated and referred to active membrane area.

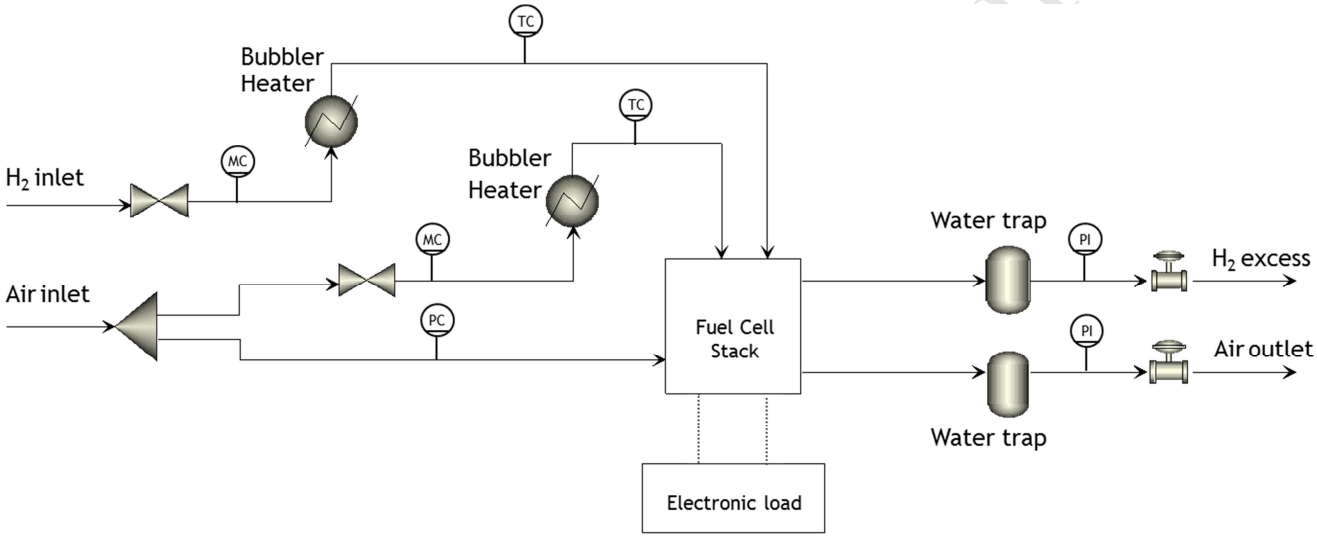

Figure 1. Experimental fuel cell set-up (MC: Gas Mass flow controller; PC: pressure controller: TC: temperature controller; PI: pressure indicator).

3. Results

The ionic liquid [HSO_3-BVIm][TfO] was respectively copolymerized with the methacrylic monomer, MMA [CH_2=C(CH_3)$COOCH_3$], and the fluorinated monomer, hPFSVE [F_2C=$CFOCF_2CF(CF_3)CF_2CF_2SO_3H$], in order to obtain flat polymer membranes with enhanced features. MMA was selected as standard monomer while hPFSVE was employed because of its chemical inertness and ionic conductivity, due to the presence of fluorine atoms and sulfonic groups. Table 1 shows the compositions employed for membrane synthesis in terms of molar IL: monomer (M) ratio (membranes are named

according to the relative molar percentage of MMA or hPFSVE employed in feeding composition regardless the amount of photoinitiator and crosslinker used, 5 and 2 wt%, respectively, or as 100 mol% in the absence of MMA and hPFSVE). Both ionic liquid and monomers seemed to be chemically compatible which resulted into thin-film homogenous membranes (Figure 2). As discussed later, only the composition based on 40 mol% of hPFSVE posed limitations for the preparation of a total membrane area of 5 cm^2 with unavoidable breakage during processing and thus this configuration was discarded for PEMFC tests.

Table 1. Starting membrane compositions (IL: ionic liquid; M: monomer MMA or hPFSVE).

Composition Name	[IL] / [M]
100 mol% IL	-
5 mol% MMA	19.0
10 mol% MMA	9.0
10 mol% hPFSVE	9.0
20 mol% hPFSVE	4.0
30 mol% hPFSVE	2.3
40 mol% hPFSVE	1.5

Schemes 1 and 2 show the schematic representation of the photoinduced copolymerizations of the IL with MMA and hPFSVE monomers, respectively.

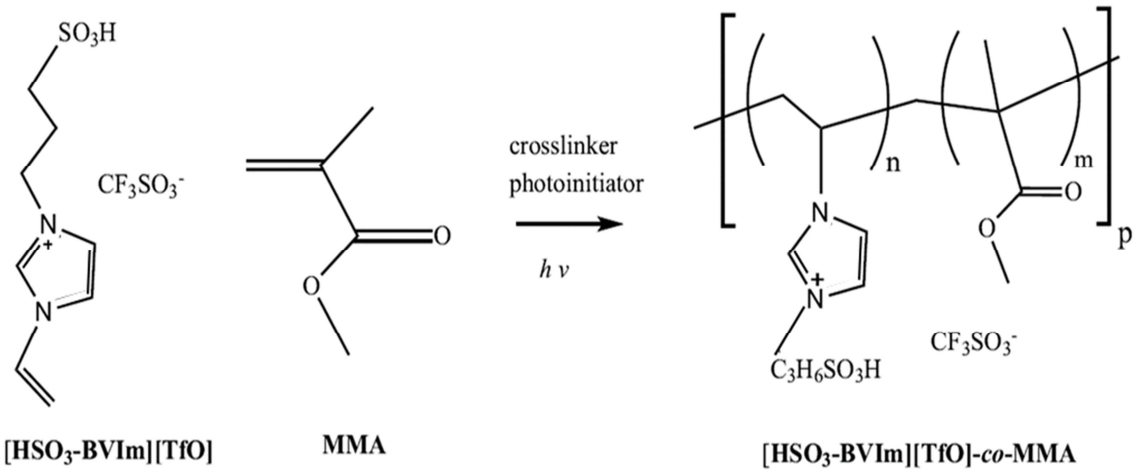

Scheme 1. Photochemical copolymerization reaction of the ionic IL [HSO_3-BVIm][TfO] and MMA.

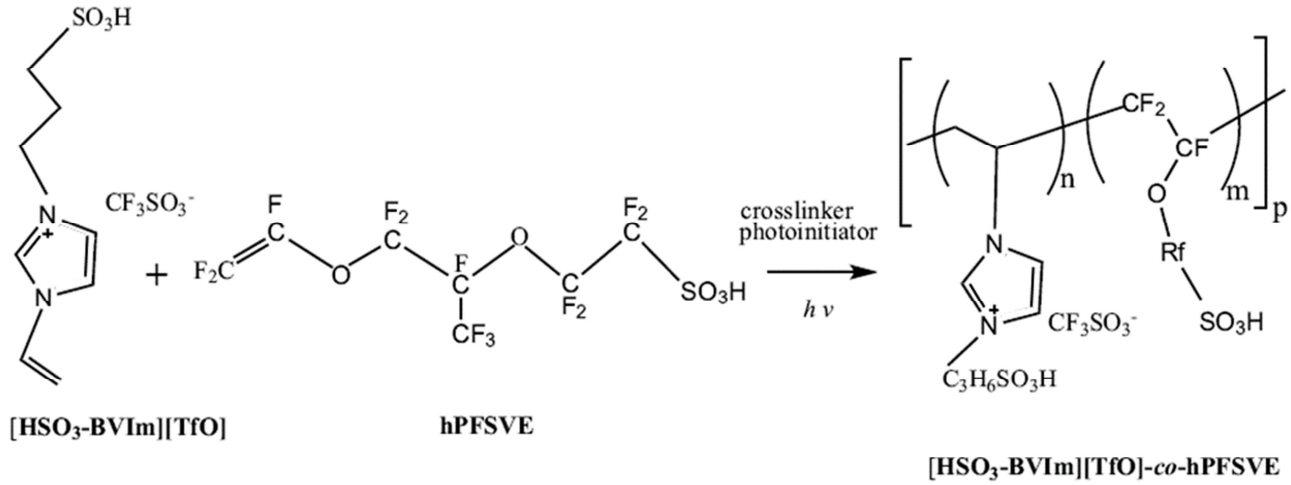

Scheme 2. Photochemical copolymerization reaction between the IL [HSO_3-BVIm][TfO] and the fluorinated monomer hPFSVE.

[HSO_3-BVIm][TfO]-based polymer membranes, in the absence and in the presence of the MMA and PFSVE comonomers, were obtained by photopolymerization. After peeled off, these membranes were characterized by microscopy, IR spectroscopy and

thermogravimetry analysis. Their electrochemical properties (conductivities and water uptakes) were also studied.

SEM analysis

Figure 2 displays the SEM images of the resulting membranes prepared from different compositions, specifically from (A) 100 mol% IL, (B) 80 mol% IL - 20 mol% fluorinated monomer hPFSVE and (C) 90 mol% IL - 10 mol% MMA. SEM analysis reveals that dense structures with no detectable pore at the limits of electron microscopy were obtained regardless the composition employed. Polymer membranes based on IL only and based on IL and MMA offered transparent aspects and were flexible, while those containing IL and hPFSVE presented translucent yellowish color (photographs in Figure 2) and behaved as less flexible. In addition, mapping analysis for fluorine and sulphur, which are present in the both the IL and the fluorinated monomer, was performed on the cross-sectional area of the membranes. The images display homogenous distribution of these elements and apparently no segregated phases were formed (See Supplementary Material). Thus, the synthesis method described in section 2.3 enables the manufacture of solid flat membranes of variable composition and thickness with no further purification required. Membranes were synthesized using a 2.5x 2.5 cm^2 glass mold and then were cut to be adjusted to the set-up membrane area of the fuel cell system (5 cm^2).

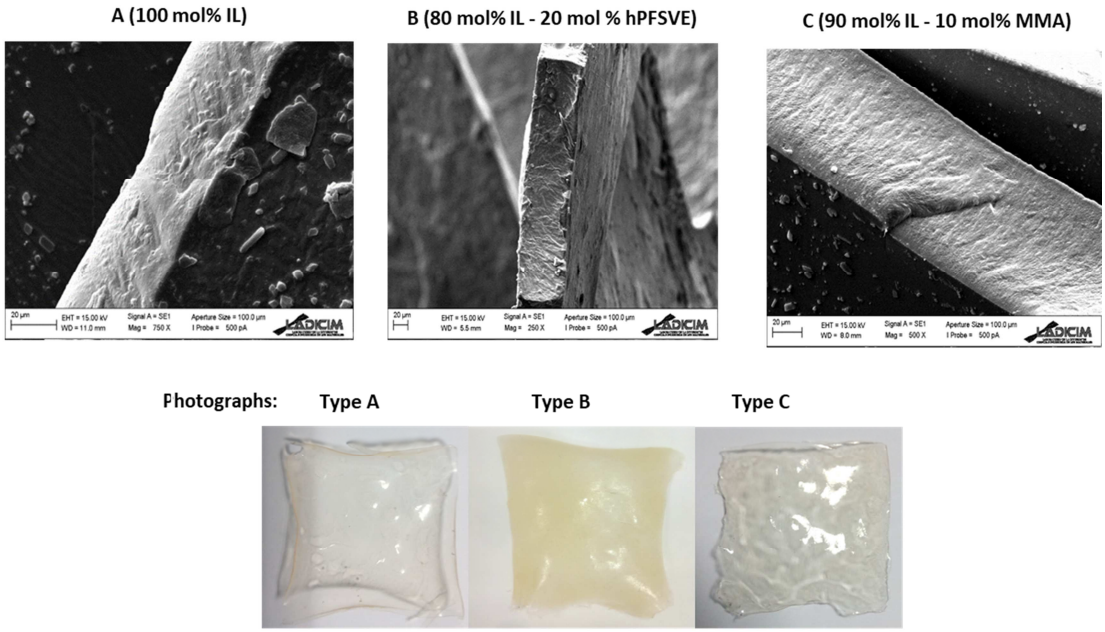

Figure 2. SEM images and photographs of representative membranes (with resulting area of over 5 cm^2): A) 100 mol% IL, B) 80 mol% IL - 20 mol% hPFSVE and C) 90 mol% IL - 10 mol% MMA.

ATR-FTIR analysis

The ATR-FTIR spectra of representative membranes, the IL monomer (bulk IL in non-polymerized form), MMA and hPFSVE comonomers and the crosslinker (glycerol dimethacrylate) are presented in Figure 3. The changes upon copolymerization are clearly noted by the characteristic band at 1655 cm^{-1} arising from the C=C vibration in [HSO_3-BVIm][TfO] IL. At this wavenumber, the peak is very pronounced for the bulk form of the IL. For the copolymerized membranes prepared from all compositions (Table

1), this peak is quite attenuated due to the conversion of the IL into the PIL form after UV curing time (30 min), confirming the success of the copolymerization. The frequency at 1638 cm^{-1} in the spectra of the crosslinker and MMA monomer (Figure 3.A) also corresponds to C=C vibration bands. These peaks disappear in the spectra of the copolymerized membranes (Figures 3.B and 3.C) since they are consumed in the copolymerization reactions according to Scheme 1. The band at 1716 cm^{-1} is attributed

to C=O stretching motions in ester functions and is characteristic of MMA monomer. Specifically, in the spectra of the membranes obtained after copolymerization of the IL with MMA, this peak clearly increases as the MMA concentration rises from 0 to 10 mol% MMA (Figure 3.B). The bands noted in the 2875-3145 cm^{-1} range are assigned to C-H and O-H stretching motions. Other characteristic peaks of the ionic liquid include those centered at 1276 and 1220 cm^{-1}, which correspond to symmetric CF_3 and asymmetric SO_3 stretching vibrations, respectively, while the band at 1026 cm^{-1} arises from symmetric SO_3 stretching [41]. Other peaks of hPFSVE monomer are observed at 1050 cm^{-1} (assigned to SO_3), 3300–3500 cm^{-1} (OH in SO_3H), 1200–1220 cm^{-1} (symmetric S=O), 1100–1240 cm^{-1} (C-F), 960–980 cm^{-1} (C-O-C) [42]. The comparison of the spectra of the resulting membranes (for all compositions) with that of the bulk ionic liquid in non-polymerized form shows broader and more pronounced peaks in the 3200-3500 cm^{-1} range (corresponding to OH stretching of water molecules) for the copolymerized membranes, indicating a higher moisture content in the membrane. These findings are in agreement with the thermogravimetric analysis of the membranes presented in the following section. For sake of clarity, only the ATR-FTIR spectrum of the poly([HSO_3-BVIm][TfO]-*co*-hPFSVE) membrane prepared at 10 mol% of hPFSVE has been included in Figure 3.C. The other spectra of membranes prepared from 20, 30 and 40 mol% of hPFSVE follow similar trends with varying peak areas due to different hPFSVE concentrations (see Supplementary Material).

Finally, Figure 4 includes the comparison of the ATR-FTIR spectra obtained for both surfaces of synthesized membranes at representative compositions (membranes prepared from 100 mol% IL, 10 mol% MMA and 20 mol% hPFSVE, respectively). During the membrane preparation process, the slurry resulting from the mixing of monomers, crosslinker and photoinitiator is spread over a glass surface and then exposed to UV light for *in situ* photopolymerization. The polymerized membranes exhibit homogenous surfaces on both sides, namely the surface of the membrane facing UV irradiation (Side

A) and the surface of the membrane facing glass (Side B). The ATR-FTIR spectra (Figure 3) offer the same profiles for both sides with no significant differences.

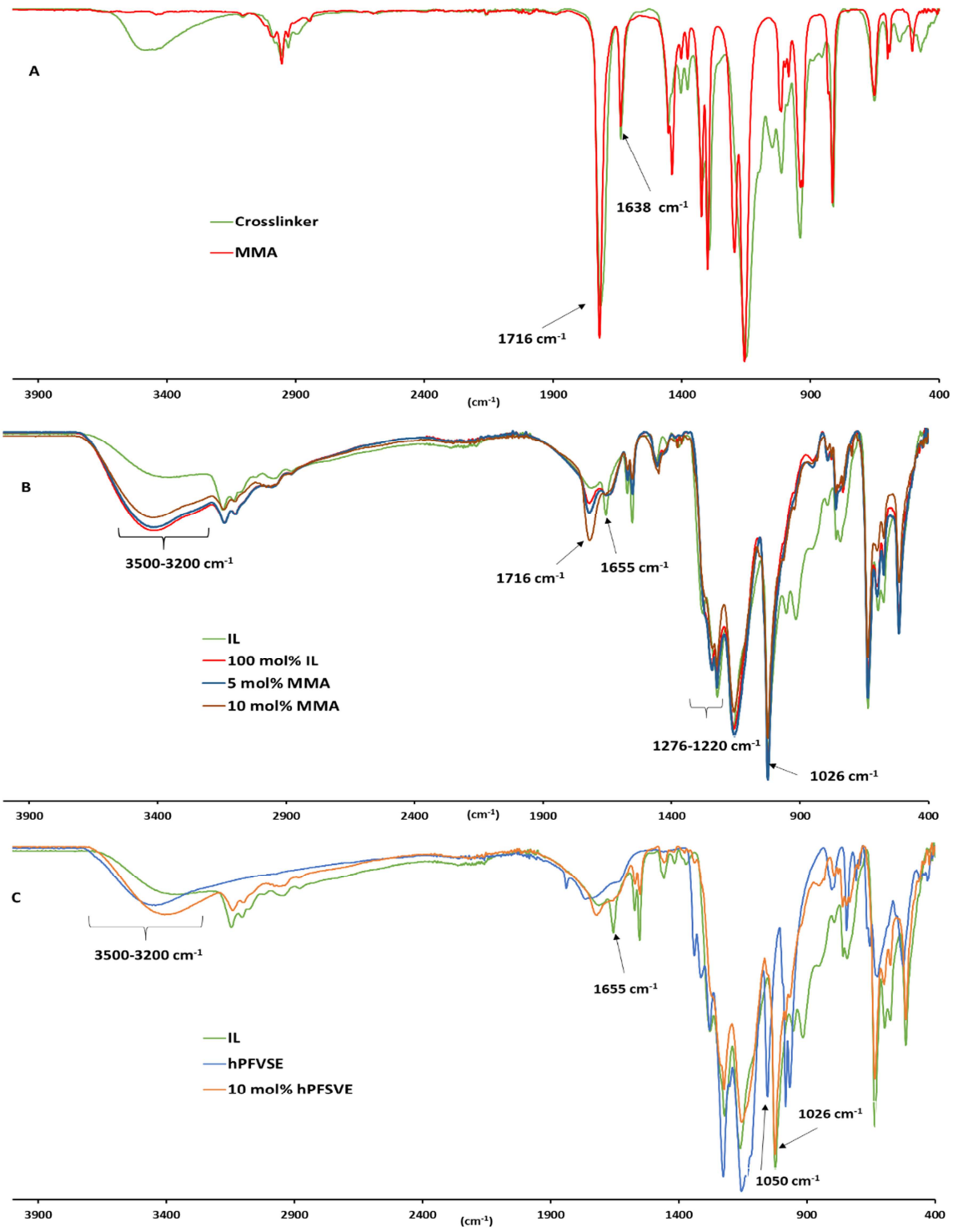

Figure 3. ATR-FTIR spectra of: A) Crosslinker (glycerol dimethacrylate) and MMA; B) bulk IL and copolymerized membranes (100 mol% IL, 5 and 10 mol% MMA); C) bulk IL, hPFSVE monomer and copolymerized membrane from 10 mol% hPFSVE.

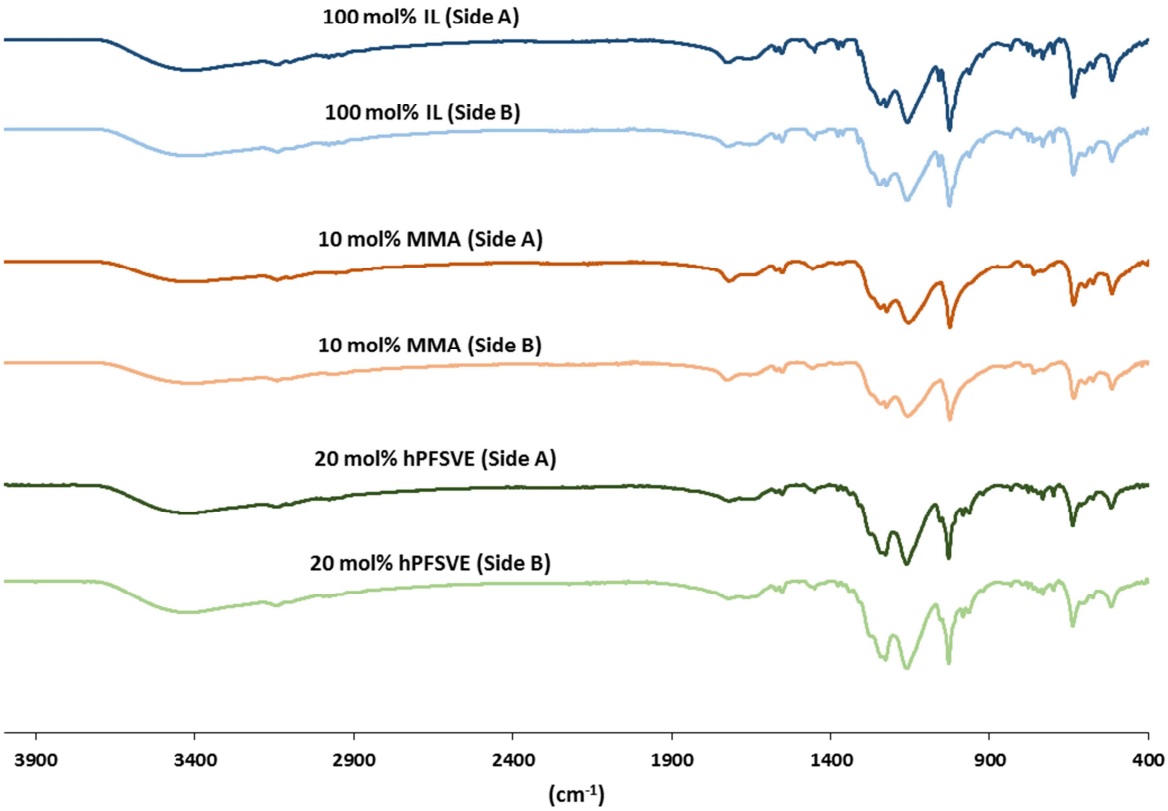

Figure 4. Comparison of ATR-FTIR spectra of both surfaces of membranes: sides A (side facing UV irradiation) and B (side facing glass substrate) of membranes prepared with 100 mol% IL, 10 mol% MMA and 20 mol% hPFSVE, respectively.

Thermogravimetric analysis

Figure 5 displays the TGA thermograms of the bulk IL (in liquid phase), the membrane based on 100 mol% IL and the membranes resulting from the copolymerization of IL with the respective MMA and hPFSVE comonomers. The results (T_1 and T_2 onset and degradation temperatures) are listed in Table 2. TGA thermograms of all membranes undergo a degradation process in several stages with similar patterns, while that of the non-polymerized IL offers one-step degradation process. Up to 150 ºC, the weight loss is most likely the result of physically absorbed water in the membranes. As seen in Table 2, the weight loss associated to this temperature is relatively high for all the membranes, which can be explained by the fact that polymer membranes present a well-organized

structure with hydrophilic domains of nanometer size in which water can be retained. In comparison, the non-polymerized IL only contains < 1 wt% of water. From 150 ºC, two significant weight loss stages are observed for all membranes with associated onset temperatures T_1 and T_2 as indicated in Table 2. T_1 onset ranges from 229 to 247 ºC for membranes based on PIL and poly(IL-*co*-MMA). In the case of membranes based on 10-20 mol% hPFVSE, T_1 was found at ca. 225 ºC, while for those prepared from 30 and 40 mol% of hPFVSE, T_1 is close to 200 ºC or below. In addition, the relative weight losses are significantly higher within the range T_1-T_2 (W_1) for membranes prepared with hPFSVE content equal to and greater than 20 mol% IL, with weight losses higher than 30 wt%. For the other compositions, W_1 remains lower than 24 %, and the higher relative weight loss (W_2) occurs from T_2 until the temperature (T_3) at which TGA thermograms start to down to the final residue. This would imply that increasing amounts of fluorinated monomer would lead to higher weight losses at lower temperatures, affecting thermal stability, due to losses of SO_2 and SO_3 from CF_2SO_3H groups [42]. TGA patterns are similar when comparing the results obtained for the membrane prepared at 100 mol% of IL with those synthesized at 5 and 10 mol%, but it is worth noting that membranes copolymerized with MMA offer the highest T_1 onset temperatures, and display better thermal stability versus membranes copolymerized with hPFSVE.

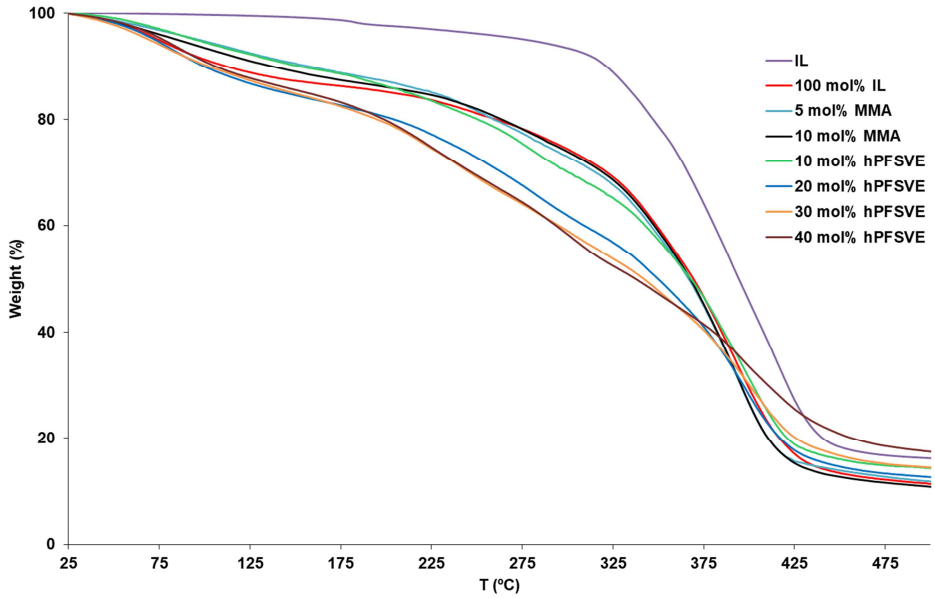

Figure 5. TGA thermograms of bulk IL and membranes prepared at different compositions of MMA and hPFSVE monomers.

Table 2. Results of TGA analysis of bulk IL and synthesized copolymers (T: onset temperatures; W: associated weight losses).

Composition Name	*Weight loss at 150 ºC (%)*	T_1 (ºC)	W_1 (%)	T_2 (ºC)	w_2 (%)	T_3 (ºC)
Bulk IL	0.8	329	70.9	-	-	457
100 mol% IL	12.8	229	14.2	325	55.8	456
5 mol% MMA	9.9	234	22.3	341	46.7	428
10 mol% MMA	11.0	247	18.1	340	49.8	432
10 mol% hPFSVE	9.8	225	23.6	338	42.8	440
20 mol% hPFSVE	15.5	224	30.9	362	29.8	434
30 mol% hPFSVE	15.1	203	38.3	374	21.1	427
40 mol% hPFSVE	14.3	199	39.9	380	18.1	441

Water uptake

Membranes were washed with water in order to monitor possible weight losses. First, membrane samples were dried under vacuum and then washed with water and dried

under the same conditions. On the other hand, water uptake was determined with new samples according to the procedure described in section 2. Table 3 presents the results obtained in both tests. The weight losses can be considered negligible, showing than membrane were not soluble in water. Synthesized membranes offered high water uptake, especially hPFSVE-based membranes. Membranes prepared from 100 mol% IL, 5 mol% MMA and 10 mol% MMA, respectively, displayed a water uptake higher than 30 %, while those obtained from hPFSVE offered water uptakes higher than 40 % at 10 and 20 mol% hPFSVE, respectively. The water uptakes for membranes at 30 mol% and 40 mol% offered too high water uptake percentages, leading to membranes with unacceptable dimensional change. In comparison with the reported values for Nafion® under the same conditions [44], the synthesized membranes displayed higher water uptakes (18 % for Nafion®-117).

Table 3. Weight loss and water uptake of membranes.

Composition name	Weight loss (%)	Water uptake (%)
100 mol% IL	1.1	33.2
5 mol% MMA	1.3	34.7
10 mol% MMA	0.4	32.6
10 mol% hPFSVE	2.0	41.7
20 mol% hPFSVE	2.1	46.7
30 mol% hPFSVE	2.4	66.9
40 mol% hPFSVE	2.7	80.1

Ionic conductivity in dry and wet conditions

Ionic conductivity measurements of the synthesized membranes were performed in an *ex situ* purpose-built cell as described in section 2.4. Figure 6 displays the conductivity of all membranes in dry and wet conditions obtained by using the ohmic resistance values from respective Bode plots (the same Y-scale is presented in Figures 6.A and 6.B in order to better reflect the general ionic conductivity enhancement in wet conditions in comparison with dry conditions). According to the results, in dry conditions, the

conductivity varies from 10^{-5} S.cm^{-1} for the membrane achieved from 100 mol% of [HSO_3-BVIm][TfO] to 10^{-2} S.cm^{-1} for the copolymerized membranes with hPFSVE. Intermediate values of 10^{-3} S.cm^{-1} were obtained for membranes resulting from the copolymerization of IL with MMA. As also observed in Figure 6, for all the given compositions, ionic conductivity increases over temperature in the 25-90 ºC range, with the exception of that prepared at 40 mol% of hPFSVE at 90 ºC, at which a drop in ionic conductivity was noted. Increasing temperatures are expected to induce higher ion mobility with consequent enhanced ionic conductivities. The larger increase in ionic conductivity with temperature in dry conditions is experienced by the membrane from 100 mol% of IL. Under wet conditions, all membranes presented conductivities in the order of 10^{-2} S.cm^{-1}. In comparison with membranes in dry conditions, the ionic conductivity increase under wet conditions is more significant for the membranes containing MMA and for those based only on IL in comparison with the improvement observed by those containing hPFSVE, which already show high conductivity under both dry and wet conditions. The high conductivity of the polymer membranes is explained by the presence of sulfonic groups (-SO_3H^-) as side chains in the imidazolium cation of the IL, which favors proton mobility and exchange. In addition, the high water content retained in the membrane structure according to the results observed with the TGA analysis can help to increase proton mobility through the H bonds formed by ions and water [45]. The ionic conductivity of the copolymerized membranes with hPFSVE is enhanced by the presence of additional sulfonic groups, displaying the highest values both in dry and wet conditions. It is worth noting that high conductivities were achieved by hPFSVE-based membranes up to 30 mol% hPFSVE at room temperature. Remarkably, the conductivity of the membrane based on 10 mol% hPFSVE reached $1.29 \cdot 10^{-2}$ Scm^{-1} and $4.19 \cdot 10^{-2}$ Scm^{-1} at 25 ºC in dry and water conditions, respectively. The membranes achieved from other compositions also displayed conductivities of ca. 10^{-2} Scm^{-1} at 25 ºC in wet conditions. These results are better than those reported by Li

et al. [47] from the *in situ* conventional radical copolymerization of MMA with 1-butyl-3-methylimidazolium hexafluorophosphate leading to gel polymer electrolytes with ionic conductivity of 10^{-3} S·cm^{-1} at 25 °C.

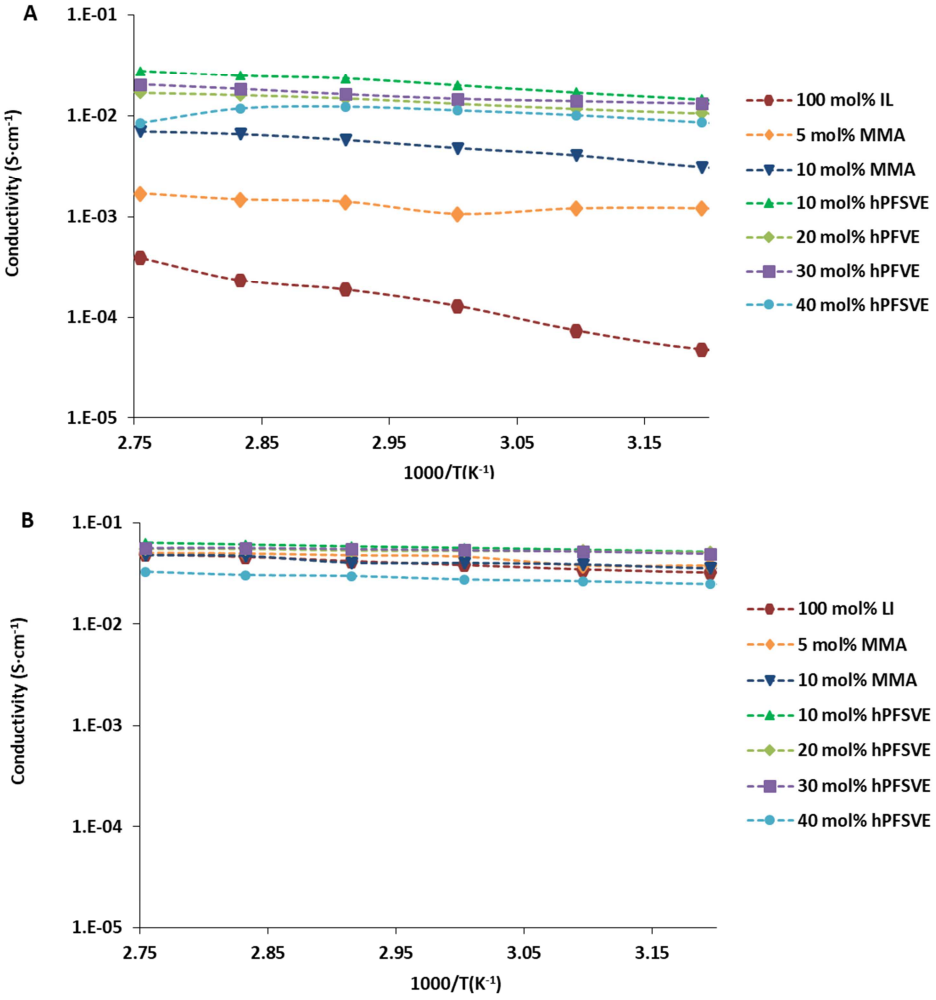

Figure 6. *Ex situ* conductivity measurements of synthesized membranes in (A) dry conditions and (B) wet conditions.

Fuel Cell Performance

The performances of all membranes except that formed by 40 mol% of hPFSVE were assessed in a PEM fuel cell device, since it was not possible to obtain a manageable membrane for a total surface membrane of 5 cm^2 (active cell area) and thus this configuration was discarded for PEMFC tests. Since most composition membranes showed similar conductivities (ca. 10^{-2} S.cm^{-1}), fuel cell operation was performed using

humidified gases to study the behavior of these membranes at optimal conditions. The synthesis method allows the membrane thickness to be adjusted for set-up requirements. The cell system is equipped with a pneumatic actuator that ensures a satisfactory contact pressure between the internal components of the cell. For PEMFC tests, membranes with thickness of around 350 µm were prepared so that they could withstand pressure contact induced by the pneumatic actuator.

Figure 7 displays the fuel cell performances of the poly(IL-*co*-hPFSVE) and poly(IL-*co*-MMA) membranes, which in turn are compared with that of the membrane with 100 mol% of polymerizable IL. As it can be observed, the addition of MMA into the synthesis process both at 5 and 10 mol% leads to higher power performances in comparison with those of the 100 mol% IL membrane. The maximum power density output was achieved with the poly(IL-*co*-MMA) membrane with 45.76 $mW.cm^{-2}$ and an associated current of 128 $mA.cm^{-2}$. PMMA has been previously employed as organic matrix in polymer gel electrolytes with resulting enhanced ionic conductivity [46]. This improvement was found to be the result of the effect of PMMA on the dissociation of the salt present in gel electrolytes.

Regarding poly(IL-*co*-hPFSVE) membranes, the performance is also clearly improved at 10 mol% of hPFSVE in comparison with the poly(IL), generating almost 30 % higher power output, with a total maximum power density of 28.12 $mW.cm^{2}$. hPFSVE monomer holds sulfonic groups that can contribute to the improvement of ionic conductivity. In comparison with MMA-based membranes, membranes including hPFSVE were less flexible and, for contents higher than 10% of hPFSVE, they became damaged after use, possibly presenting crossover issues during fuel cell operation. In fact, poly(IL-*co*-hPFSVE) membranes with hPFSVE concentrations of equal to and higher than 20 mol% resulted in lower power performances compared to that of PIL membrane (Figure 7.C).

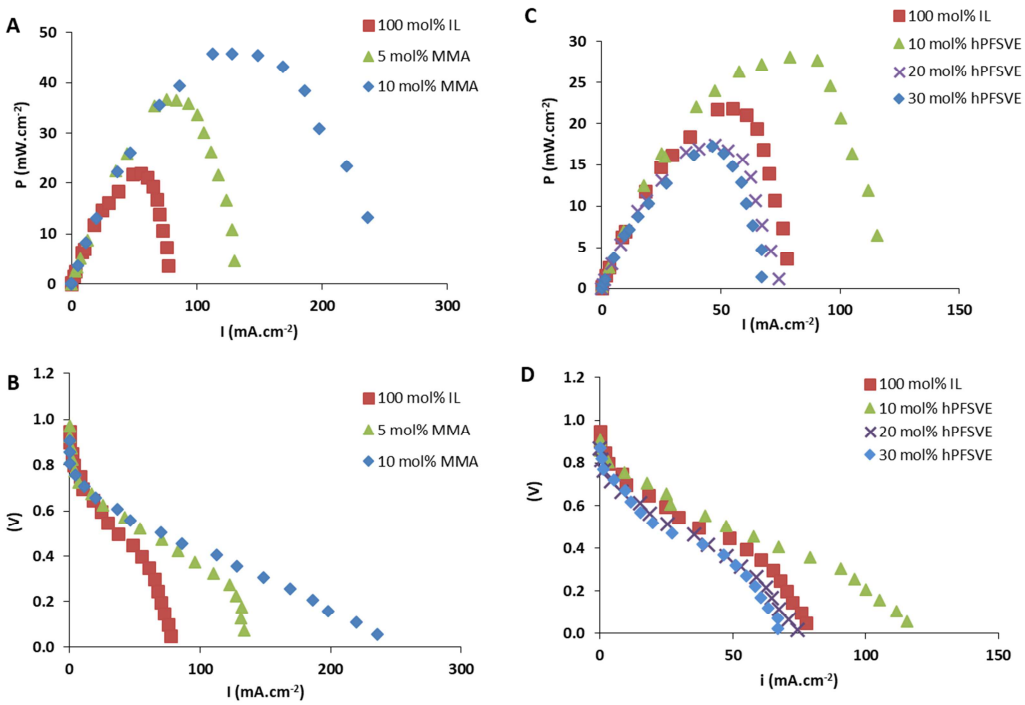

Figure 7. Comparison of the performance of poly(IL-*co*-hPFSVE) and poly([IL-*co*-MMA) membranes with the poly(IL) membrane in a PEMFC): A, C) power curves ; B, D) polarization curves.

According to the EIS measurements, both copolymer membranes of poly(IL-*co*-MMA) and poly(IL-*co*-hPFSVE) offered high conductivities at room temperature and even in dry conditions (in the order of 10^{-2} S·cm^{-1} for membranes containing hPFSVE). Thus, the differences in fuel cell performance cannot be explained only by considering ionic conductivity since other factors such as the mechanical stability and thickness need to be taken into consideration. On the other hand, the power performance obtained by Nafion® in the same system and under similar conditions was reported as high as 68 mW.cm^{-2} at 25 °C [48], which is not far from the best result obtained in this work. However, it is worth noting that the thickness of Nafion® membrane employed in that work is much lower than the average thickness obtained within the studied copolymer membranes. In this sense, further works will need to consider the synthesis of [HSO3-

BVIm][TfO]-based copolymer membranes with higher mechanical stability at lower thickness to increase power performances.

Conclusions

Novel copolymer electrolyte membranes based on the ionic liquid [HSO_3-BVIm][TfO] and monomers such as methyl methacrylate (MMA) and perfluoro-3,6-dioxa-4-methyl-7-octane sulfonic acid (hPFSVE) were developed as proton exchange membranes. The successful photoinduced copolymerization reactions between the ionic liquid and the respective monomers in the presence of a crosslinker and a photoinitiator were confirmed with ATR-FTIR. The resulting membranes displayed high ionic conductivity, within the 10^{-3} - 10^{-2} $S.cm^{-1}$ range, both in dry and wet conditions at room temperature. The maximum power performance was obtained with poly(IL-*co*-MMA) and poly(IL-*co*-hPFSVE) membranes at 10 mol% of MMA and hPFSVE, respectively, with maximum power outputs of 45.76 and 28.12 $mW.cm^{-2}$. Copolymer electrolytes at optimal MMA or hPFSVE concentrations clearly outperformed the pristine [HSO_3-BVIm][TfO]-based polymeric membrane in terms of power output. TGA analysis showed that the new membranes showed degradation temperatures higher than 200 ºC, which is suitable for PEMFC application and that their structures are capable of retaining high water content inside their structure. Further works will consider the synthesis of [HSO_3-BVIm][TfO]-based copolymer membranes with higher mechanical stability at lower thickness to increase power performance.

Acknowledgments

This research was supported by the projects SOE1/P1/E0293 (INTERREG SUDOE /FEDER, UE) and CTQ2015-66078-R. E. Tojo thanks the Xunta de Galicia (REGALIs Network, ED431D 2017/06) for funding and the research support services of the

University of Vigo (CACTI) for the NMR and MS divisions. V.M. Ortiz-Martínez is supported by the Spanish Ministry of Science, Innovation and Universities (grant 'Juan de la Cierva-Formación' ref. FJCI-2017-32404).

References

[1] E.H. Majlan, D. Rohendi, W.R.W. Daud, T. Husaini, M.A. Haque, Electrode for proton exchange membrane fuel cells: A review, Renew. Sustain. Energy Rev. 89 (2018) 117–134. doi:10.1016/j.rser.2018.03.007.

[2] O.Z. Sharaf, M.F. Orhan, An overview of fuel cell technology: Fundamentals and applications, Renew. Sustain. Energy Rev. 32 (2014) 810–853. doi:10.1016/J.RSER.2014.01.012.

[3] J. Wang, H. Wang, Y. Fan, Techno-Economic Challenges of Fuel Cell Commercialization, Engineering. 4 (2018) 352–360. doi:10.1016/J.ENG.2018.05.007.

[4] Y. Tanaka, Development of the MIRAI Fuel Cell Vehicle. In: K. Sasaki, H.W. Li, A. Hayashi, J. Yamabe, T. Ogura, S., Lyth (eds) Hydrogen Energy Engineering. Green Energy and Technology. Springer, Tokyo, 2016, Chapt. 10, pp 461-475.

[5] S. Maity, S. Singha, T. Jana, Low acid leaching PEM for fuel cell based on polybenzimidazole nanocomposites with protic ionic liquid modified silica, Polymer (Guildf). 66 (2015) 76–85. doi:10.1016/J.POLYMER.2015.03.040.

[6] D.W. Shin, M.D. Guiver, Y.M. Lee, Hydrocarbon-Based Polymer Electrolyte Membranes: Importance of Morphology on Ion Transport and Membrane Stability, Chem. Rev. 117 (2017) 4759–4805. doi:10.1021/acs.chemrev.6b00586.

[7] S. Subianto, M. Pica, M. Casciola, P. Cojocaru, L. Merlo, G. Hards, D.J. Jones, Physical and chemical modification routes leading to improved mechanical properties of perfluorosulfonic acid membranes for PEM fuel cells, J. Power

Sources. 233 (2013) 216–230. doi:10.1016/J.JPOWSOUR.2012.12.121.

[8] J. Kerres, F. Schönberger, A. Chromik, T. Häring, Q. Li, J.O. Jensen, C. Pan, P. Noyø, N.J. Bjerrum, Partially Fluorinated Arylene Polyethers and Their Ternary Blend Membranes with PBI and H 3 PO 4. Part I. Synthesis and Characterisation of Polymers and Binary Blend Membranes ~, (n.d.). doi:10.1002/fuce.200800011.

[9] B.K. Nath, A. Khan, J. Chutia, Composite plasma polymerized sulfonated polystyrene membrane for PEMFC, Mater. Res. Bull. 70 (2015) 887–895. doi:10.1016/J.MATERRESBULL.2015.06.028.

[10] K.H. Lee, S.Y. Lee, D.W. Shin, C. Wang, S.H. Ahn, K.J. Lee, M.D. Guiver, Y.M. Lee, Structural influe~ce of hydrophobic diamine in sulfonated poly(sulfide sulfone imide) copolymers on medium temperqture PEM fuel cell, Polymer (Guildf). 55 (2014) 1317–1326. doi:10.1016/j.polymer.2013.09.030.

[11] S. Singha, T. Jana, Effect of composition on the properties of PEM based on polybenzimidazole and poly(vinylidene fluoride) blends, Polymer (Guildf). 55 (2014) 594–601. doi:10.1016/j.polymer.2013.12.021.

[12] J. Walkowiak-Kulikowska, J. Wolska, H. Koroniak, Polymers application in proton exchange membranes for fuel cells (PEMFCs), Phys. Sci. Rev. 2 (2017). doi:10.1515/psr-2017-0018.

[13] R. Sood, S. Cavaliere, D.J. Jones, J. Rozière, Electrospun nanofibre composite polymer electrolyte fuel cell and electrolysis membranes, Nano Energy. 26 (2016) 729–745. doi:10.1016/j.nanoen.2016.06.027.

[14] J. Zhang, Y. Tang, C. Song, J. Zhang, Polybenzimidazole-membrane-based PEM fuel cell in the temperature range of 120-200 °C, J. Power Sources. 172 (2007) 163–171. doi:10.1016/j.jpowsour.2007.07.047.

[15] N.N. Krishnan, D. Joseph, N.M.H. Duong, A. Konovalova, J.H. Jang, H.-J. Kim,

S.W. Nam, D. Henkensmeier, Phosphoric acid doped crosslinked polybenzimidazole (PBI-OO) blend membranes for high temperature polymer electrolyte fuel cells, J. Memb. Sci. 544 (2017) 416–424. doi:10.1016/J.MEMSCI.2017.09.049.

[16] N. Li, Z. Cui, S. Zhang, S. Li, F. Zhang, Preparation and evaluation of a proton exchange membrane based on oxidation and water stable sulfonated polyimides, J. Power Sources. 172 (2007) 511–519. doi:10.1016/J.JPOWSOUR.2007.07.069.

[17] Q. Yuan, P. Liu, G.L. Baker, Sulfonated polyimide and PVDF based blend proton exchange membranes for fuel cell applications, J. Mater. Chem. A. 3 (2015) 3847–3853. doi:10.1039/c4ta04910a.

[18] H.R. Allcock, R.M. Wood, Design and synthesis of ion-conductive polyphosphazenes for fuel cell applications: Review, J. Polym. Sci. Part B Polym. Phys. 44 (2006) 2358–2368. doi:10.1002/polb.20864.

[19] R.-Q. Fu, J.-J. Woo, S.-J. Seo, J.-S. Lee, S.-H. Moon, Sulfonated polystyrene/polyvinyl chloride composite membranes for PEMFC applications, J. Memb. Sci. 309 (2008) 156–164. doi:10.1016/J.MEMSCI.2007.10.013.

[20] S. Elakkiya, G. Arthanareeswaran, K. Venkatesh, J. Kweon, Enhancement of fuel cell properties in polyethersulfone and sulfonated poly (ether ether ketone) membranes using metal oxide nanoparticles for proton exchange membrane fuel cell, Int. J. Hydrogen Energy. 43 (2018) 21750–21759. doi:10.1016/J.IJHYDENE.2018.04.094.

[21] E. Raphael, C.O. Avellaneda, B. Manzolli, A. Pawlicka, Agar-based films for application as polymer electrolytes, Electrochim. Acta. 55 (2010) 1455–1459. doi:10.1016/j.electacta.2009.06.010.

[22] J. Yu, B. Yi, D. Xing, F. Liu, Z. Shao, Y. Fu, H. Zhang, Degradation mechanism of

polystyrene sulfonic acid membrane and application of its composite membranes in fuel cells, Phys. Chem. Chem. Phys. 5 (2003) 611–615. doi:10.1039/b209020a.

[23] M. Díaz, A. Ortiz, I. Ortiz, Progress in the use of ionic liquids as electrolyte membranes in fuel cells, J. Memb. Sci. 469 (2014) 379–396. doi:10.1016/j.memsci.2014.06.033.

[24] M. Galiński, A. Lewandowski, I. Stępniak, Ionic liquids as electrolytes, Electrochim. Acta. 51 (2006) 5567–5580. doi:10.1016/J.ELECTACTA.2006.03.016.

[25] M. Watanabe, M.L. Thomas, S. Zhang, K. Ueno, T. Yasuda, K. Dokko, Application of Ionic Liquids to Energy Storage and Conversion Materials and Devices, Chem. Rev. 117 (2017) 7190–7239. doi:10.1021/acs.chemrev.6b00504.

[26] C. Iojoiu, O. Danyliv, F. Alloin, Ionic Liquids and Polymers for Battery and Fuel Cells, in: Mod. Synth. Process. React. Fluorinated Compd. Prog. Fluor. Sci., 2016: pp. 465–497. doi:10.1016/B978-0-12-803740-9.00016-0.

[27] R. HAGIWARA, J.S. LEE, Ionic Liquids for Electrochemical Devices, Electrochemistry. 75 (2007) 23–34. doi:10.5796/electrochemistry.75.23.

[28] J. Le Bideau, L. Viau, A. Vioux, Ionogels, ionic liquid based hybrid materials, Chem. Soc. Rev. 40 (2011) 907–925. doi:10.1039/c0cs00059k.

[29] H. Zhang, W. Wu, J. Wang, T. Zhang, B. Shi, J. Liu, S. Cao, Enhanced anhydrous proton conductivity of polymer electrolyte membrane enabled by facile ionic liquid-based hoping pathways, J. Memb. Sci. 476 (2015) 136–147. doi:10.1016/j.memsci.2014.11.033.

[30] J. Mališ, P. Mazúr, J. Schauer, M. Paidar, K. Bouzek, Polymer-supported 1-butyl-3-methylimidazolium trifluoromethanesulfonate and 1-ethylimidazolium trifluoromethanesulfonate as electrolytes for the high temperature PEM-type fuel

cell, Int. J. Hydrogen Energy. 38 (2013) 4697–4704. doi:10.1016/j.ijhydene.2013.01.126.

[31] A. Eguizábal, J. Lemus, M.P. Pina, On the incorporation of protic ionic liquids imbibed in large pore zeolites to polybenzimidazole membranes for high temperature proton exchange membrane fuel cells, J. Power Sources. 222 (2013) 483–492. doi:10.1016/j.jpowsour.2012.07.094.

[32] M. Suckow, M. Roy, K. Sahre, L. Häußler, N.K. Singha, B. Voit, F. Böhme, Synthesis of polymeric ionic liquids with unidirectional chain topology by AB step growth polymerization, Polymer (Guildf). 111 (2017) 123–129. doi:10.1016/J.POLYMER.2017.01.063.

[33] H. He, H. Chung, E. Roth, D. Luebke, D. Hopkinson, H. Nulwala, K. Matyjaszewski, Low glass transition temperature poly(ionic liquid) prepared from a new quaternary ammonium cationic monomer, Polym. Adv. Technol. 26 (2015) 823–828. doi:10.1002/pat.3529.

[34] J. Steinkoenig, F.R. Bloesser, B. Huber, A. Welle, V. Trouillet, S.M. Weidner, L. Barner, P.W. Roesky, J. Yuan, A.S. Goldmann, C. Barner-Kowollik, Controlled radical polymerization and in-depth mass-spectrometric characterization of poly(ionic liquid)s and their photopatterning on surfaces, Polym. Chem. 7 (2016) 451–461. doi:10.1039/C5PY01320H.

[35] Y. Gnanou, D. Taton, Macromolecular Engineering by Controlled Radical Polymerization, in: Handb. Radic. Polym., 2002. doi:10.1002/0471220450.ch14.

[36] N. Samadi, N. Mohammadnezhad, A. Abbas Matin, H. Valizadeh, Ionic liquid loaded hollow fiber membrane as a solid-phase microextraction fiber; application in determination of aromatic hydrocarbons in water samples, J. Chem. Pharm. Res. 8 (2016) 491–502.

[37] C. Detrembleur, A. Debuigne, M. Hurtgen, C. Jérôme, J. Pinaud, M. Fèvre, P. Coupillaud, J. Vignolle, D. Taton, Synthesis of 1-vinyl-3-ethylimidazolium-based ionic liquid (co)polymers by cobalt-mediated radical polymerization, Macromolecules. 44 (2011) 6397–6404. doi:10.1021/ma201041s.

[38] J.R. Nykaza, A.M. Savage, Q. Pan, S. Wang, F.L. Beyer, M.H. Tang, C.Y. Li, Y.A. Elabd, Polymerized ionic liquid diblock copolymer as solid-state electrolyte and separator in lithium-ion battery, Polymer (Guildf). 101 (2016) 311–318. doi:10.1016/j.polymer.2016.08.100.

[39] E. Andrzejewska, Photoinitiated polymerization in ionic liquids and its application, Polym. Int. 66 (2017) 366–381. doi:10.1002/pi.5255.

[40] S.M. Chen, T.L. Wang, P.Y. Chang, C.H. Yang, Y.C. Lee, Poly(ionic liquid) prepared by photopolymerization of ionic liquid monomers as quasi-solid-state electrolytes for dye-sensitized solar cells, React. Funct. Polym. 108 (2016) 103–112. doi:10.1016/j.reactfunctpolym.2016.06.006.

[41] M. Díaz, A. Ortiz, M. Isik, D. Mecerreyes, I. Ortiz, Highly conductive electrolytes based on poly([HSO3-BVIm][TfO])/[HSO3-BMIm][TfO] mixtures for fuel cell applications, Int. J. Hydrogen Energy. 40 (2014) 11294–11302. doi:10.1016/j.ijhydene.2015.03.109.

[42] M. Colpaert, M. Zatoń, G. Lopez, D.J. Jones, B. Améduri, Revisiting the radical copolymerization of vinylidene fluoride with perfluoro-3,6-dioxa-4-methyl-7-octene sulfonyl fluoride for proton conducting membranes, Int. J. Hydrogen Energy. 43 (2018) 16986–16997. doi:10.1016/J.IJHYDENE.2018.03.153.

[43] N. Wagner, T. Kaz, K.A. Friedrich, Investigation of electrode composition of polymer fuel cells by electrochemical impedance spectroscopy, Electrochim. Acta, 53 (2008) 7475–7482. doi:10.1016/J.ELECTACTA.2008.01.084.

[44] M. Colpaert, M. Zaton, V. Ladmiral, D. Jones, J. Rozière, B. Ameduri, Crosslinked terpolymers of vinylidene fluoride, perfluoro-3,6-dioxa-4-methyl-7-octene sulfonyl fluoride, and cure site monomers for membranes in PEMFC applications, Polym. Chem. 10 (2019) 2176–2189. doi:10.1039/C9PY00188C.

[45] Z. Wojnarowska, J. Knapik, M. Díaz, A. Ortiz, I. Ortiz, M. Paluch, Conductivity mechanism in polymerized imidazolium-based protic ionic liquid [HSO3-BVIm][OTf]: Dielectric relaxation studies, Macromolecules. 47 (2014) 4056–4065. doi:10.1021/ma5003479.

[46] R. Kumar, S.S. Sekhon, Effect of molecular weight of PMMA on the conductivity and viscosity behavior of polymer gel electrolytes containing NH4CF3SO3, Ionics (Kiel). 14 (2008) 509–514. doi:10.1007/s11581-008-0209-0.

[47] Z. Li, J. Jiang, G. Lei, D. Gao, Gel polymer electrolyte prepared by in situ polymerization of MMA monomers in room temperature ionic liquid, Polym. Adv. Technol. 2006 (17) 604–607. doi:10.1002/pat.760.

[48] M. Díaz, A. Ortiz, M. Vilas, E. Tojo, I. Ortiz, Performance of PEMFC with new polyvinyl-ionic liquids based membranes as electrolytes, Int. J. Hydrogen Energy, 2014 (39) 3970–3977. doi:10.1016/j.ijhydene.2013.04.155.

Highlights

- Photopolymerization of ionic liquid [HSO_3-BVIm][TfO] with MMA and fluorinated (hPFSVE) monomers.
- Poly(IL-*co*-MMA) and poly(IL-*co*-hPSVE) as new electrolyte membranes in PEM fuel cells
- Significant conductivity of poly(IL-co-MMA) and poly(IL-*co*-hPSVE) in dry and wet conditions
- Enhanced power performance of copolymer membranes compared with pristine poly(ionic liquid)